Sustainable Water Resources Management (2020) 6:54
https://doi.org/10.1007/s40899-020-00415-6

ORIGINAL ARTICLE

Fluoride-bearing groundwater in the complex terminal aquifer (a case study in Hassi Messaoud area, southern Algeria): hydrochemical characterization and spatial distribution assessed by indicator kriging

Rabah Kechiched[1] · Imed Eddine Nezli[2] · Atif Foufou[1,3] · Mohamed Salah Belksier[1] · Slimane Abdeldjabbar Benhamida[2,4] · Rabah Djeghoubbi[1] · Nacereddine Slamene[5] · Ouafi Ameur-zaimeche[1]

Received: 26 December 2019 / Accepted: 1 June 2020 / Published online: 8 June 2020

Abstract

According to the World Health Organisation (WHO), the human consumption of water containing a high concentration of fluoride (> 1.5 mg/l) can increase significantly many health problems such as dental and skeletal fluorosis. This study investigates fluoride abundance, origin, and its spatial distribution in groundwater from Complex Terminal (CT) aquifer in Hassi Messaoud area (Southern Algeria) where the CT water constitutes the main source of drinking water with a high daily intake. Available water wells were sampled and analysed on their major physico-chemical parameters including fluoride content. Hydrochemical characterization was constrained using the Durov diagram together with a PCA statistical treatment. The saturation indices were computed and used to track fluoride origin. The spatial distribution of fluoride in the studied aquifer was mapped by indicator kriging (IK). The results show that fluoride content ranges from 1.6 to 2.9 mg/l (average = 2.1 ± 0.4 mg/l) exceeding WHO drinking water standards. The Durov diagram, PCA and SI indicate that water acquires mineralization principally by leaching of evaporite minerals. Furthermore, SI evidences that fluoride concentration in water increases with $CaCO_3$ precipitation leading to CaF_2 dissolution. IK spatial distribution allows estimating the probability of not exceeding (2.1 mg/l) critical threshold. The cross-validation displays good performance of IK estimation (mean error = 0.05; mean standard error = 0.09). The obtained map shows a low to moderate probability of not exceeding the selected threshold in the whole aquifer. Therefore, the use of CT water for human consumption poses a risk to public health. These results can be used in water management framework and for selecting an ideal position to drill new boreholes for drinking water.

Keywords Fluoride · Indicator kriging · Saturation indices · Dental fluorosis · Terminal complex aquifer · Hassi Messaoud · Algeria

✉ Rabah Kechiched
rabeh21@yahoo.fr; kechiched.ra@univ-ouargla.dz

Imed Eddine Nezli
imedinezli@yahoo.fr

Atif Foufou
foufou_atif@yahoo.fr

Mohamed Salah Belksier
mouhbelksier@yahoo.fr

Slimane Abdeldjabbar Benhamida
slimbenha@gmail.com

Rabah Djeghoubbi
djeghoubbi.rabah@yahoo.fr

Nacereddine Slamene
zft_nasro@yahoo.fr

Ouafi Ameur-zaimeche
ouafigeology@gmail.com

[1] Laboratoire des Réservoirs Souterrains: Pétroliers, Gaziers et Aquifères, Université Kasdi Merbah Ouargla, 30000 Ouargla, Algeria

[2] Laboratoire de Géologie de Sahara, Université Kasdi Merbah Ouargla, 30000 Ouargla, Algeria

[3] Earth and Universe Sciences Department, Ziane Achour-Djelfa University, 17000 Djelfa, Algeria

[4] Agence Nationale des Ressources Hydriques (ANRH) – Direction Sud-Ouargla, 30000 Ouargla, Algeria

[5] École Nationale Supérieure Agronomique d'Alger, El Harrache, Algeria

Introduction

Groundwater in the Algerian Sahara represents the main source of water for domestic, agricultural and industrial uses. The Hassi Messaoud oil field is well known in Algeria by its intense industrial activity of hydrocarbon upstream and downstream. Nearby, the city of Hassi Messaoud which is situated 650 km southeastern Algiers, dependents on groundwater supply especially from the Terminal Complex (CT) aquifer. The demand for water increases at a quick rate as a result of the development of needs by habitation and to satisfy the industrial request. Therefore, ensuring the quantity and the quality of water supply can often appear a real challenge.

The CT aquifer in this area is mainly formed by sandy and gavels deposits of Mio-Pliocene and carbonates of Senonian rocks (UNESCO 1972), and is a part of a large aquifer system called Western Sahara Aquifer System (NWSAS). This system is shared by three countries (Algeria, Tunisia, and Libya) with over a one million km^2 of lateral extension and a notable variation of the thickness from one region to another (UNESCO 1972). In this aquifer, waters often display discharge temperatures around ~ 25 °C and are highly mineralized thus it needs to be treated before its uses. In addition, water as everywhere in the Algerian Sahara, is characterized by high concentrations of fluoride which exceed the standards of World Health Organization (WHO) (≥ 1.5 mg/l) for drinking water as reported in many studies (e.g. Youcef and Achour 2001, 2004; Guendouz et al. 2003; Djellouli et al. 2005; Messaitfa 2008; Nezli et al. 2009). The fluoride (F^-) has an atomic number of 9 with a molecular mass of 19 g/mol and is characterized by high reactivity. The inorganic fluoride occurrence is usually free in fluid solutions (Wedepohl 1974). According to the WHO (2017), fluoride has a protective effect which increases with content up to about 2 mg/l in drinking water while the minimum concentration is around 0.5 mg/l. On the contrary, high fluoride content (≥ 1.5 mg/l) has an undesirable effect and it accelerates dental and skeletal fluorosis. Furthermore, this risk may increase depending on drinking water intake which is the most likely high in warmer and arid areas such as Algerian Sahara. Therfore, good knowledge of its spatial distribution into the aquifer is required.

This study is performed on groundwater from the CT aquifer below the Hassi Messaoud city and is aimed at (1) investigating fluoride contents from CT wells that are used for water supply (2) studying the distribution of fluoride in the aquifer using indicator kriging (IK). IK will be applied on a set of available data and it helps to perform a probability map of not exceeding a threshold of fluoride. The selected threshold here is represented by the median value of fluoride content in investigated samples (Me = 2.1 mg/l) corresponding to a critical fluoride content in drinking water which accelerates significantly dental and skeletal fluorosis. IK method which is a nonlinear geostatistical interpolation is more suitable in our case study than ordinary kriging (OK) which has some limitations such as requiring an assumption of a normal distribution of data (Krige 1951; Matheron 1963; Lloyd and Atkinson 2001). IK can provide a solution to that required assumption by transforming continuous to indictor data based on a threshold that can be defined by a median value (e.g. Lloyd and Atkinson 2001; Mohammadpour et al. 2019). Note that IK is applied by Journel (1983) to carry out spatial distribution for interpolation and it is favoured here, for studying fluoride distribution regarding 2.1 mg/l without any precondition of the distribution of data (Jang et al. 2008). In the literature, IK is largely used for mapping of heavy metals in groundwater such as arsenic (Lee et al. 2007) and water salinities (Belkesier et al. 2018). Fluoride data will be transformed into binary coding (0, 1) regarding the 2.1 mg/l value. In other words, all interpolations will be between 0 and 1, and the obtained map will show the probability of not exceeding the indicator value of fluoride in water. The obtained map allows classifying different zones in the aquifer regarding their probabilities of not exceeding 2.1 mg/l. If a low probability of not exceeding 2.1 mg/l threshold is recorded, water can therefore represent a risk to health and needs defluoridation before its consumption. The obtained map can act as a help of decision-making for water management and for selecting the ideal position to drill new wells for drinking water in the future.

Study area

Geology

The Hassi Messaoud city is located 650 km southeastern of Algiers, about 86 km from Ouargla City and 350 km from the Algerian–Tunisian border (Fig. 1). This area is well known in Algeria and in worldwide by its large oil and gas industry. Therefore, the population has concentrated in this city nearby working sites and is estimated at around 45,000 inhabitants in 2008. The studied area lies between latitudes 31° 39′ 16.47″ N and 31°45′ 12.47″ N, and longitudes from 6° 2′ 11.47″ E to 6° 4′ 41.30″ E. The climate is arid with low precipitations (average monthly: 0.1–7 mm), and high temperatures particularly in summer which may exceed 45 °C.

The geology of Hassi Messaoud area is well known because of many geological works that are conducted during exploration activity by oil companies such as SONATRACH and its partners. A synthesis of the petroleum geology in Algeria which includes detailed geological background of

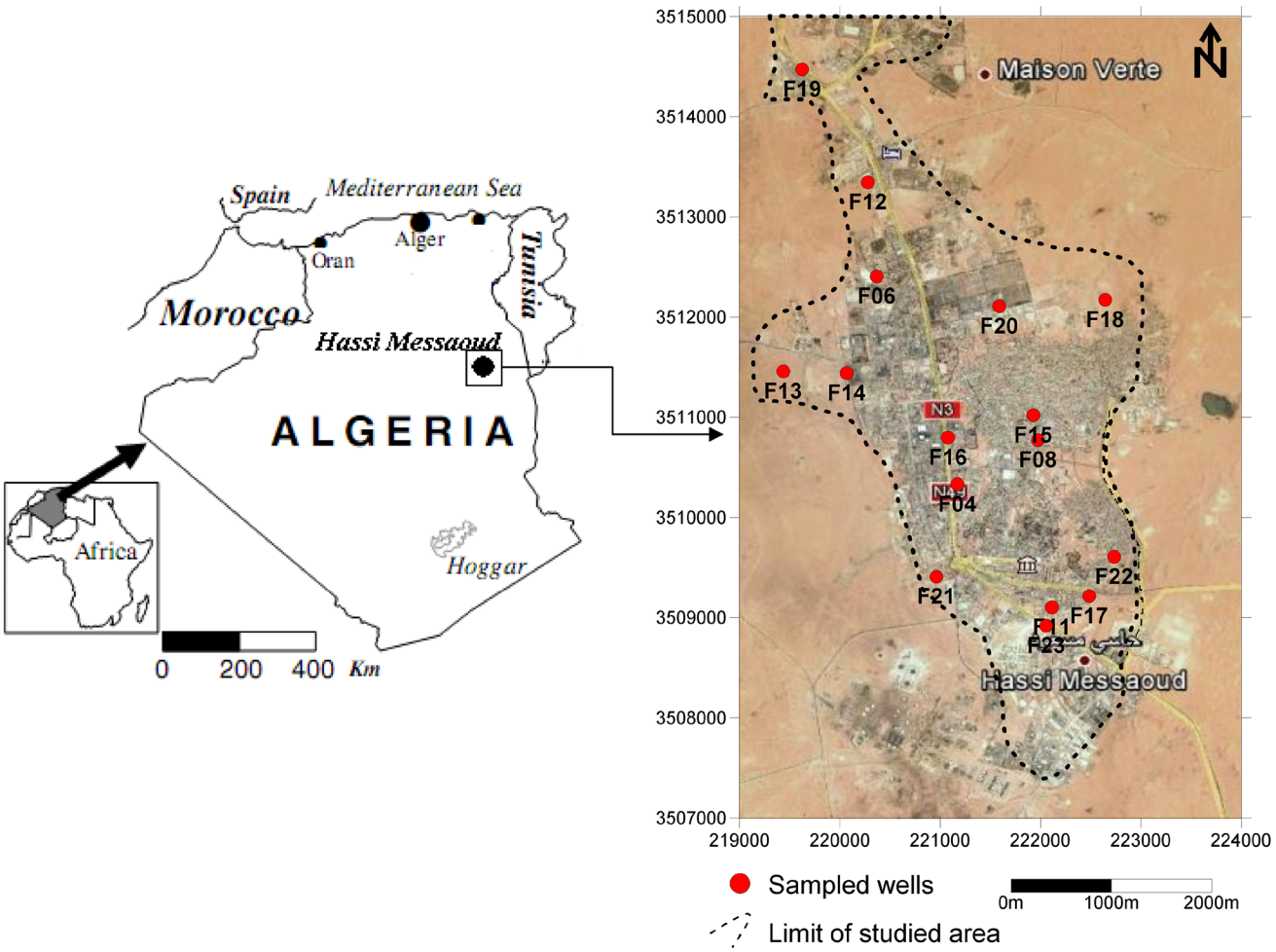

Fig. 1 Location map of the study area and sampled wells from the Complex Terminal aquifer in the Hassi Messaoud city

Hassi Messaoud and other oil–gas basins is published by Sonatrach-Schlumberger (WEC 2007). According to this report and other unpublished documents of drilling logs (Sonatrach 2002), the Hassi Messaoud area is considered to belong within to intracratonic basin of Oued Mya. Lithologies are composed of a succession of about 4393 m thickness. The sedimentary layers are aged from Cambrian to Quaternary, and are characterized by the absence of Silurian, Devonian, Carboniferous and Permian due to the Hercynian unconformity (WEC 2007).

Hydrogeology

The Hassi Messaoud area as the Northern Sahara of Algeria contains a system of two important aquifers which extends to Tunisia and Libya hosting considerable quantities of paleowater according to isotopic data (e.g. Edmunds and Gaye 1997; Guendouz et al. 1997; Edmunds et al. 2003). In this system, two main aquifers can be distinguished: (1) the confined and discharged Continental Intercalary (CI) represented by a multi-layer aquifer including Albian, Barremian and Neocomian formations. The Albian aquifer is the most exploited representing the main target of drilling wells for water in Northern Sahara of Algeria. (2) The Complex Terminal (CT) overlays the Continental Intercalaire (CI) and is formed mainly by Mio-Pliocene sands and Senonian carbonates. In the study area, the Senonian carbonates have a reduced thickness as great Oriental Erg where the Mio-Pliocene reservoir is exploited for water. The flow direction of water in this aquifer is from Tinrhert Plateau in the South towards the Chotts region in North (Fig. 2) (Guendouz et al. 2003).

Data and methods

Samples and laboratory analysis

Although the Hassi Messaoud area represents an industrial zone that attracts the population, only a few investigations

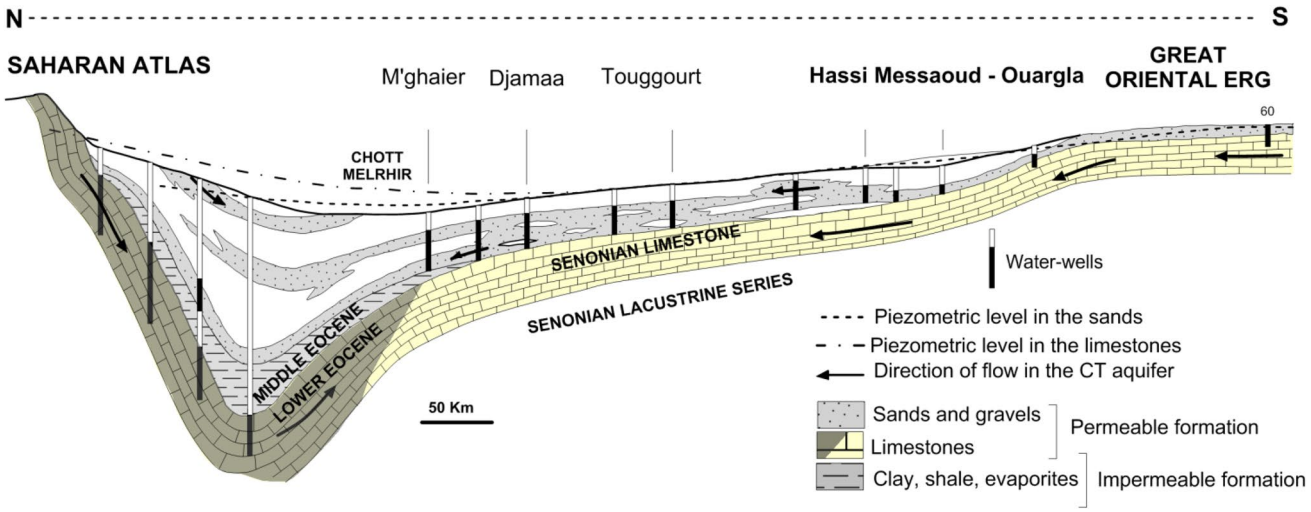

Fig. 2 Hydrogeological cross section of the Complex Terminal aquifer in Algeria (after UNSCO 1972; Guendouz et al. 2003)

were conducted on hydrochemical issues (e.g. Bouselsal 2017; Sahri et al. 2017). The high intake of groundwater from CT aquifer to human consumption especially in the summer period may increase health problems due to the concentration of some elements such as fluoride. Therefore, this study aims to discuss fluoride concentration together with major physic-chemical parameters. The wells that are used for water supply in the city were sampled and sixteen water samples were collected from the CT aquifer displaying relatively good spatial distribution for a nonparametric geostatistical study (see Fig. 1). Physico-chemical analyses were performed in laboratories of the national agency of water resources (ANRH) and the Algerian waters (ADE) of Ouargla following Rodier (1996) standards. The concentrations of Na^+ and K^+ were determined using a flame spectrophotometer (PFP 7, JENWAY). F^-, SO_4^{2-} and Cl^- were recorded by a spectrophotometer machine (DR2000, HACH) and HCO_3^- was determined by titration. Mg^{2+} and Ca^{2+} were analysed by complexometric titration using Ethylenediaminetetraacetic acid (EDTA) protocol (Mg^{2+} = TH-Ca^{2+}). Other parameters were measured "in situ" directly after sampling such as Electrical Conductivity (EC) using a multiparameter. Based on the percentage ion-balance, the overall test of water analysis accuracy indicates that samples have charge imbalances less than ± 6% except one sample (F19 = ± 6.69%). The Durov diagram was used to determine water facies and the chemistry origin of water. Note that the Durov diagram helps to carry out a graphical representation of the water chemistry by plotting cations and anions into separate ternary diagrams (Durov 1948; Lloyd and Heathcote 1985; Belkhiri et al. 2010).

Saturation index

In natural solutions, water mineral interactions represent the main control of water alkalinity (e.g. Morel 1983; Drever 1988). The carbonate alkalinity (Alc_c) is a part of total alkalinity represented by HCO_3^- and CO_3^{2-} anions where calcite is the main mineral affected. Saturation state regarding preponderant minerals can be recognized by thermodynamic models and computed by ‹‹ Phreeqci.v.3, Parkhurst and Appelo 2013›› software using its database (Phreeqci.dat). The calculation of the saturation index as SI = log (Q)/log (Kps) of dissolved minerals at temperature of 25 °C in studied water samples based on the law of extended Debye–Hückel. A thermodynamic equilibrium state is considered when SI ranges between − 0.5 and + 0.5. Lower SI values than − 0.5 indicate unsaturation, whereas those higher than + 0.5 reflect oversaturation. The saturation indices were used to clarify possible origins of fluoride in studied samples.

Statistical analysis

Data were statistically analysed using the following methods: (1) descriptive statistics to determine data characteristics such as central tendency and dispersion parameters. (2) Bivariate statistics were used to perform a correlation matrix with the help of calculating Pearson ratios of correlation. (3) Multivariate statistical analysis was performed using Principal Component Analysis (PCA), which is considered an appropriate method related to factor analysis. It used on exploratory data analysis to carry out predictive models according to the correlation between variables in

a multidimensional space. PCA consists in data projection into n dimensional space (scatter plot), i.e. a dimensionality-reduction technique that transforms high-dimensional datasets into smaller-dimensional subspace. This simplification helps the interpretation of different relations between the studied variables and individuals. The results of a PCA are usually discussed in terms of component scores (factor scores) and loadings (Shaw 2003). In this study, PCA was applied to evidence possible associations of physicochemical parameters which may have the proxy to recognize different origins in acquiring water chemistry.

Geostatistics

Geostatistical methods have been used in different scientific disciplines, especially in earth sciences, where first applications were carried out in mining sites (e.g. Krige 1951; Matheron 1963, 1971). The fundaments basis of geostatistics has been wholly given by many authors (e.g. Matheron 1971; Chauvet 1999). Geostatistics aims at studying and characterizing spatial data where sampling coordinates are coupled with the studied variables to carry out mathematical functions that interpret the spatial variability (regionalized variables). Geostatistical interpolation methods give an ideal estimation at an un-sampled location. We define here the following vocabulary and geostatistical methods that are used in this study:

The variogram is the basic tool in the geostatistical analysis that describes the degree of spatial correlation between pairs of observations separated by a certain distance (h). In other words, the variogram $\gamma(h)$ consists in one-half of the variance of the difference between the attribute values at all points $z(x)$ and $z(x+h)$ separated by a distance (h) (Fig. 3a). The experimental variogram is calculated by the following formula:

$$\gamma(h) = \frac{1}{2N(h)} \left\{ \sum_{i=1}^{N(h)} [z(x) - z(x+h)]^2 \right\} \quad (1)$$

where $\gamma(h)$ is the semi-variogram for the distance (h); $N(h)$ is the number of pairs for observed data in each lag (h); $z(x)$ and $z(x+h)$ represent the values of studied regionalized variable in the location (x) and ($x+h$), respectively.

The experimental variograms are after fitted by theoretical models including the following parameters: nugget effect (c_0), Sill (c) and range (a). Note that each parameter has a significant role in the spatial study (Fig. 3b). The nugget effect (c_0) represents the variogram value at zero lag distance

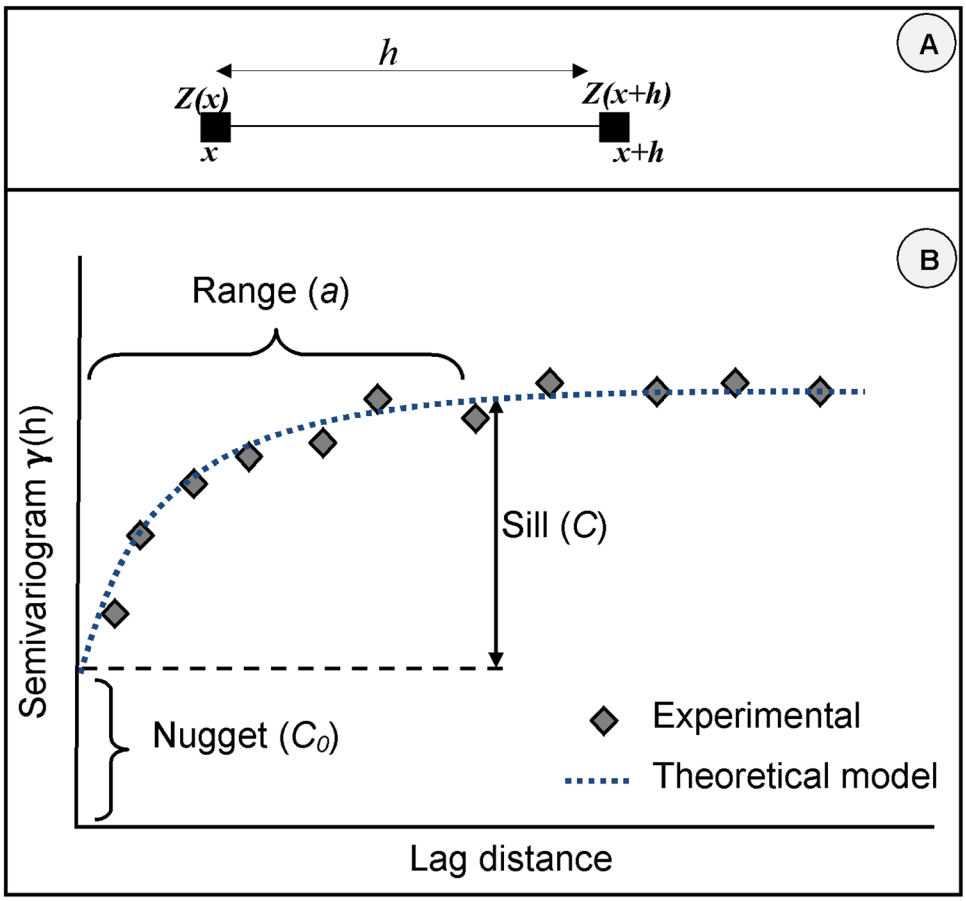

Fig. 3 **a** Graphic representation of two points for variogram calculation and, **b** Graphic representation of variogram showing the fitting parameters (Matheron 1971)

$\gamma(h=0)$ indicating the variability in very small scale than the sampling distance. Large nugget effect can be interpreted as measurement errors. The sill (c) represents the magnitude of variogram at the distance when reaching the range (a), which indicates the influence radius and the distance which measured observations are no longer correlated spatially (Fig. 3b). We denote that several mathematical models are available for fitting experimental variograms such as spherical, exponential, gaussian and linear models are founded in the literature (see Xavier 2001).

Indicator kriging (IK)

Indicator kriging (IK) is a nonparametric geostatistical method which is based on transforming measurements to binary values (0, 1) depending on if a threshold (Z_k) is exceeded or not (Goovaerts 2000). In this study, the transformation was performed according to fluoride threshold (2.1 mg/l) which represents the median value. The 2.1 mg/l fluoride threshold represents a cut-off where fluoride concentration becomes considerably harmful to human health. Indictor data were transformed for each sampling well where continuous data were converted to discrete indicator variables by giving the probability of "0" for the fluoride values exceeding the selected threshold and the probability of "1" for fluoride values that are equal or below the same selected threshold.

$$I(xi;Z_k)=\begin{cases}0 \text{ if } Z(xi) > Z_k\\ 1 \text{ if } Z(xi) \le Z_k\end{cases} \quad Z_k = 2.1 \text{ mg/l} \tag{2}$$

The variogram will be established and fitted on the newly transformed data while IK is used to create a probability map of not exceeding fluoride threshold. The mapping will be performed on a regular grid 250 m × 250 m size.

Cross-validation

The cross-validation is a procedure used to evaluate the performance of IK estimation and the fitting quality of variogram. In cross-validation, each measured data value will be removed individually and re-estimated using neighbour data. Measured and re-estimated data are after compared according to mean error (ME), average standard error (ASE), mean standard error (MSE), root square error (RMSE), mean square standard error (MSSE) and root-mean-square standardized error (RMSSE) using the following formulas from the literature (e.g. Chilès and Delfiner 1999; ESRI 2008; Ashrafzadeh et al. 2016):

$$\text{ME}=\frac{1}{n}\sum_{i=1}^{n}(Zx-Zx*) \tag{3}$$

$$\text{ASE}=\sqrt{\frac{1}{n}\sum_{i=1}^{n}\sigma^2} \tag{4}$$

$$\text{MSE}=\frac{1}{n}\sum_{i=1}^{n}\frac{(Zx*-Zx)^2}{\sigma_k} \tag{5}$$

$$\text{RMSE}=\sqrt{\frac{\sum_{i=1}^{n}(Zx-Zx*)^2}{n}} \tag{6}$$

$$\text{MSSE}=\frac{1}{n}\sum_{i=1}^{n}\frac{(Zx*-Zx)^2}{\sigma_k^2} \tag{7}$$

$$\text{RMSSE}=\sqrt{\frac{1}{n}\sum_{i=1}^{n}\frac{(Zx*-Zx)^2}{\sigma_k^2}} \tag{8}$$

Note that $Z(x)$ is the observed value, $Z(x)*$ is the re-estimated value and n represents the number of observation used. For good estimation performance, the ME and MSE should be close to zero (0) together with smaller RMSE.

Results and discussion

Elementary statistics

Main elementary statistics of physico-chemical parameters of analysed samples are given in Table 1. The pH varies between 6.6 and 7.8. Water samples display high electrical conductivities (EC from 1900 to 4890 µS/cm; average = 2758 µS/cm) associated with high standard deviation (σ = 892 µS/cm) indicating substantial variability from one sample to another. Samples show high concentrations of Ca^{2+}, Mg^{2+}, Na^{+}, SO_4^{2-} and Cl^{-} (average = 199 ± 44 mg/l, 92 ± 33 mg/l, 312 ± 205 mg/l, 660 ± 336 mg/l and 529 ± 258 mg/l, respectively (Table 1).

Major chemical composition reflects the origin of mineralization from hosting rocks in water reservoirs that are represented mainly by evaporite minerals, and minor carbonate minerals. Fluoride content varies between 1.6 and 2.9 mg/l (average = 2.1 ± 0.4 mg/l) exceeding the WHO standards for drinkable water. The obtained F^{-}contents are quite similar to those reported in other location from the Complex Terminal aquifer of northern Algerian Sahara (e.g. Messaitfa 2008; Nezli et al. 2009).

Hydrochemical characterization

Based on the Durov diagram, the studied samples from the Complex Terminal aquifer in the Hassi Messaoud are mainly plotted into the field 5 and 8 indicating that they are

Table 1 Physico-chemical parameters and descriptive statistics (all values in mg/l except electrical conductivity EC in µS/cm)

Wells	EC µS/cm	pH pH	TDS mg/l	SO_4^{2-} mg/l	Cl^- mg/l	HCO_3^- mg/l	Na^+ mg/l	K^+ mg/l	Mg^{2+} mg/l	Ca^{2+} mg/l	F^- mg/l
F04	4890	7.4	4020	1688	875	173.8	780	54	181.8	260	1.63
F06	2250	7.6	1600	430	444	128.4	300	10	81.6	132.3	2.34
F08	2800	7.8	2134	788	445	207.4	295	25.5	92.2	170	2.71
F11	2500	6.9	2000	600	431.9	180.1	200	15	79.2	236.5	2.93
F12	2000	7.8	1596	744	140	204.3	119	16.8	112.6	132.5	2.28
F13	1990	6.8	1500	525	303.9	145.2	100	15	84	192.4	2.25
F14	1900	7.0	1300	455	284.3	162.7	100	15	74.14	144.3	1.6
F15	4200	7.0	3300	1100	911.8	122	700	45	88.8	256.5	2.46
F16	2390	7.2	1500	300	492.6	180.9	200	25	67.2	216.4	1.73
F17	2230	6.7	1800	485	433.8	182.2	200	10	48	196.4	2.12
F18	2600	7.0	1800	500	534.3	145.2	300	20	79.2	184.4	2.26
F19	2200	6.6	1800	510	372.8	162.7	188	10	120	160.3	2.1
F20	3800	7.3	2988	580	1068	133.6	500	35	127.2	236.5	2.13
F21	3600	6.8	2700	800	835	162.7	500	20	88.88	264.5	1.97
F22	2020	6.9	1500	400	366	182.2	200	10	50.4	196.4	1.86
F07	–	–	–	–	–	–	–	–	–	–	1.57
Min.	1900	6.6	1300	300	140	122	100	10	48	132.3	1.6
Max.	4890	7.8	4020	1688	1068	207.4	780	54	181.8	264.5	2.9
Average	2758	7.1	2102.5	660.3	529.2	164.9	312.1	21.8	91.7	198.6	2.1
Median	2390	7	1800	525	444	162.7	200	16.8	84	196.4	2.1
Standard deviation	892.2	0.4	765.1	335.9	257.9	25.1	205.5	12.9	32.3	43.9	0.4

acquiring mineralization from the dissolution of hosting formation (Fig. 4). According to Lloyd and Heathcoat (1985), the field "5" shows that there is no dominance any cation or anion suggesting probable freshwater recharge (40% of analysed samples). The field "8" exhibits the dominance of Na^+ and Cl^- indicating the influence of basic ions exchanges on water. The field "9" represents water samples that display high saturation of Na^+ and Cl^- which is linked to halite dissolution. We denote that the last two fields represent 60% of analysed samples and it reflects the role of geological formation in acquiring mineralization of the Complex Terminal aquifer and is represented by sand and evaporites (Mio-Pliocene). The direct contact with the hosting formation conducts to the dissolution of several minerals in water (Fig. 4).

Correlation matrix

Pearson correlation ratios between physic-chemical parameters are given in Table 2. It shows high and positive correlation (r) between EC and the following elements: TDS (0.99) K^+ (0.91), Na^+ (0.98), SO_4^{2-} (0.83), Cl^- (0.90), Ca^{2+} (0.77), Mg^{2+} (0.66) (r significant at $p<0.01$).

The positive correlation between Ca^{2+} and SO_4^{2-} (0.51, r significant at $p<0.06$) is higher than that between Ca^{2+} and Mg^{2+} ($r=0.24$) suggesting that the Ca^{2+} in CT water is derived mainly from evaporites (dissolution of gypsum and anhydrite). The low and non-significant correlations between F^- versus other elements indicates that fluoride may be originated from other mineral phases and is related to different thermodynamic equilibrium of fluoride minerals as suggested by Nezli et al. (2009) and is discussed below.

Principal component analysis (PCA)

Principal Component Analysis is used here to identify the origin of water mineralization. Selected physico-chemical parameters are plotted on main components PC1, PC2 and PC3. PC1 versus PC2 and PC1 versus PC3 gather a cumulative variance of 72.06% and 65.39%, respectively (Fig. 5). Both the two last projections show one cluster of physico-chemical parameters representing the mineralization pole which consists of EC, K^+, Na^+, SO_4^{2-}, Cl^-, Ca^{2+} and Mg^{2+}. This cluster reflects the origin of water mineralization that is represented mainly by leaching of evaporites.

The F^- position against the mineralization cluster suggests that fluoridation is relatively unrelated with the dissolution of evaporites and carbonates but with other minerals containing fluoride (Fig. 5). According to Pearson's correlations and PCA analysis, the fluoride presence may be linked to other elements such as fluorine (CaF_2) and Fluor-apatite ($Ca_5(PO_4)_3F$) minerals as suggested by Nezli et al. (2009) in the CT groundwater from the Ouargla region.

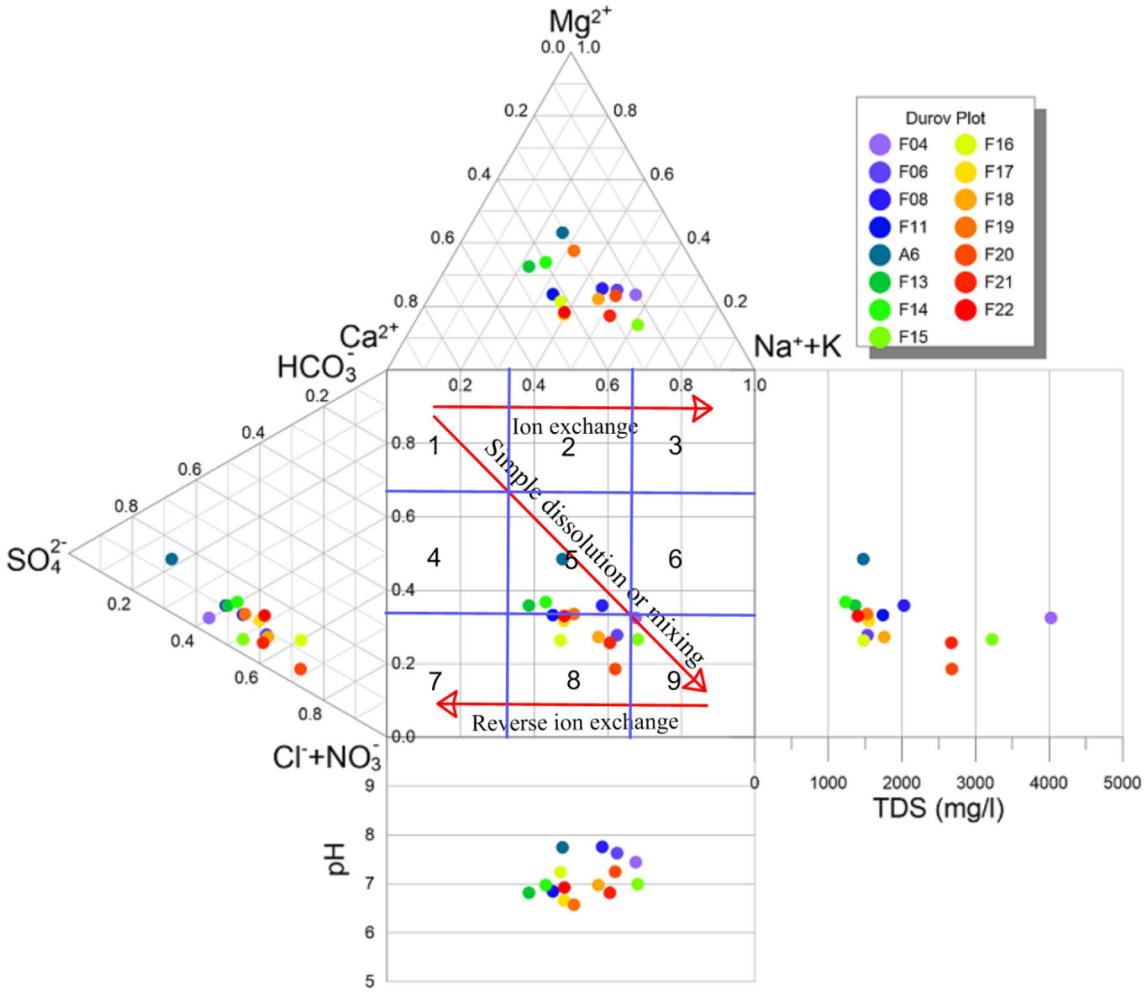

Fig. 4 The Durov plot (Lloyd and Heathcote 1985) depicting hydrochemical processes involved in the Complex Terminal of Hassi Messaoud aquifer

Table 2 Pearson's correlations between physico-chemical parameters in CT groundwater at Hassi Messaoud (significant correlations at $p < 0.05$ are marked in bold)

Variables	EC	pH	TDS	SO_4^{2-}	Cl^-	HCO_3^-	Na^+	K^+	Mg^{2+}	Ca^{2+}	F^-
EC	**1**										
pH	0.15	**1**									
TDS	**0.99**	0.13	**1**								
SO_4^{2-}	**0.83**	0.28	**0.87**	**1**							
Cl^-	**0.90**	−0.01	**0.86**	0.52	**1**						
HCO_3^-	−0.29	0.25	−0.24	0.02	−0.49	**1**					
Na^+	**0.98**	0.16	**0.96**	**0.81**	**0.89**	−0.37	**1**				
K^+	**0.91**	0.31	**0.89**	**0.82**	**0.76**	−0.20	**0.87**	**1**			
Mg^{2+}	**0.66**	0.35	**0.71**	**0.75**	0.45	−0.05	0.59	**0.67**	**1**		
Ca^{2+}	**0.77**	−0.29	**0.75**	0.51	**0.79**	−0.20	**0.72**	0.64	0.24	**1**	
F^-	−0.09	0.13	−0.04	−0.06	−0.09	0.01	−0.09	−0.14	−0.15	−0.05	**1**

Saturation indices and fluoride origin insights

The saturation indices (SI) of some common minerals are given in Table 3. It shows that waters are undersaturated with respect to evaporite minerals (gypsum, anhydrite, halite, and sylvite), indicating that these minerals are undergoing dissolution in the studied waters. However, waters are slightly saturated to equilibrium regarding calcite, aragonite

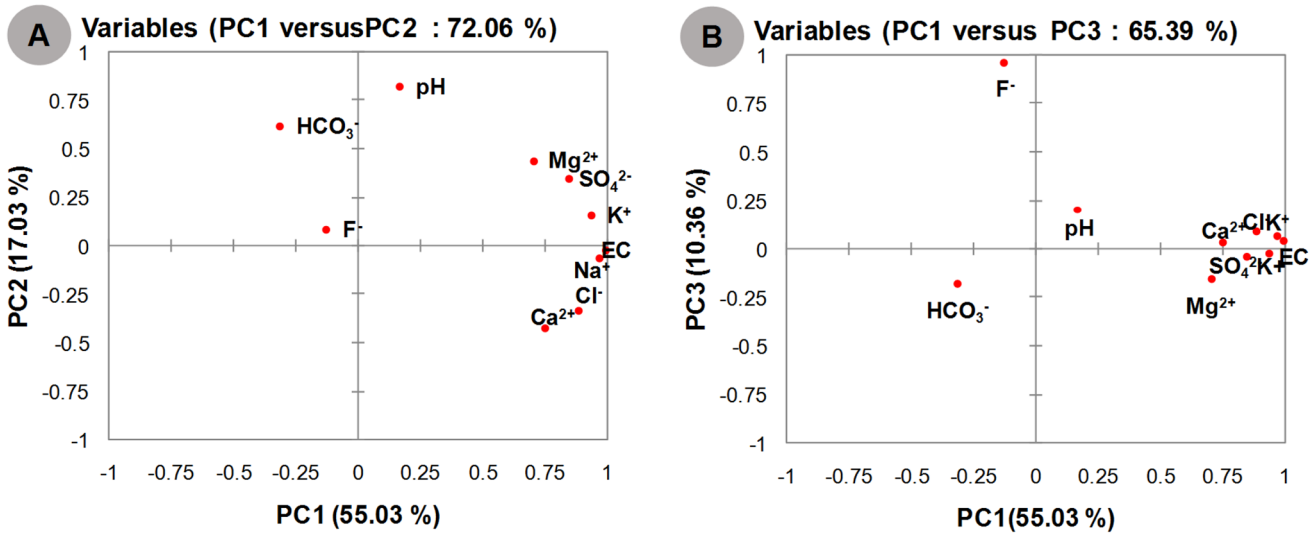

Fig. 5 Loading the factors from the PCA showing the mineralization association **a** PC1 versus PC2, **b** PC1 versus PC3

Table 3 Saturation indices with respect to main minerals and partial pressure of CO_2 in the studied water wells

Minerals	Anhydrite $CaSO_4$	Aragonite $CaCO_3$	Calcite $CaCO_3$	$CO_2(g)$ $CO_2(g)$	Dolomite $CaMg(CO_3)_2$	Fluorite CaF_2	Gypsum $CaSO_4{\cdot}2H_2O$	Halite NaCL	Sylvite KCl	$LogpCO_2$
F04	−0.72	0.16	0.30	−2.20	0.77	−0.57	−0.42	−4.86	−5.59	−3.67
F06	−1.31	0.12	0.27	−2.50	0.66	−0.28	−1.01	−5.51	−6.55	−3.96
F08	−1.03	0.50	0.64	−2.43	1.34	−0.12	−0.72	−5.53	−6.16	−3.89
F11	−0.98	−0.29	−0.14	−1.57	−0.43	0.14	−0.67	−5.70	−6.39	−3.04
F12	−1.11	0.40	0.55	−2.41	1.35	−0.36	−0.81	−6.41	−6.82	−3.88
F13	−1.07	−0.47	−0.33	−1.62	−0.68	−0.15	−0.77	−6.14	−6.53	−3.09
F14	−1.22	−0.37	−0.23	−1.72	−0.42	−0.54	−0.91	−6.16	−6.55	−3.19
F15	−0.81	−0.38	−0.24	−1.89	−0.62	−0.10	−0.51	−4.87	−5.63	−3.36
F16	−1.26	0.11	0.26	−1.96	0.35	−0.30	−0.95	−5.64	−6.10	−3.42
F17	−1.09	−0.53	−0.38	−1.36	−1.04	−0.17	−0.78	−5.69	−6.56	−2.83
F18	−1.14	−0.36	−0.21	−1.78	−0.46	−0.19	−0.84	−5.43	−6.18	−3.25
F19	−1.20	−0.76	−0.61	−1.33	−1.02	−0.34	−0.89	−5.79	−6.63	−2.8
F20	−1.08	−0.06	0.08	−2.12	0.23	−0.23	−0.78	−4.93	−5.66	−3.59
F21	−0.89	−0.37	−0.23	−1.59	−0.60	−0.24	−0.59	−5.04	−6.01	−3.06
F22	−1.16	−0.24	−0.09	−1.64	−0.44	−0.27	−0.85	−5.76	−6.63	−3.1

and dolomite (Table 3). These observations reflect water facies which is represented mainly by Cl, Na-SO_4 and less Ca water-types. It argued furthermore that water mineralization is originated mainly from the dissolution of evaporite-bearing Mio-Pliocene hosting formation and, secondly from carbonaceous rocks of Senonian rocks.

On other hand, positive Pearson's correlations that have been recorded between Ca and saturation indices of dolomite ($r=0.52$), fluorite ($r=0.42$), calcite ($r=0.40$) and, in a lesser degree with respect to gypsum ($r=0.33$) indicating that Ca is chemically controlled by carbonates and evaporite minerals. The presence of Na–SO_4 water type indicates a Ca^{2+} replacement from water by Na^+ of clayey formation in the aquifer. Furthermore, the Ca water type that is hosted especially in carbonates of Senonian rocks shows CO_2 pressure above than atmospheric pressure ($Log_{10}pCO_2=-3.5$) and is undersaturated with respect to dolomite, calcite and aragonite excepting some samples (F04, F06, F08) which show an oversaturation regarding to the same minerals together with lower CO_2 pressure to similar to atmospheric. This may be interpreted by water degassing when collecting samples (Fig. 6).

Saturation indices are also used to forecast reactive minerals in subsurface based on groundwater chemistry and to

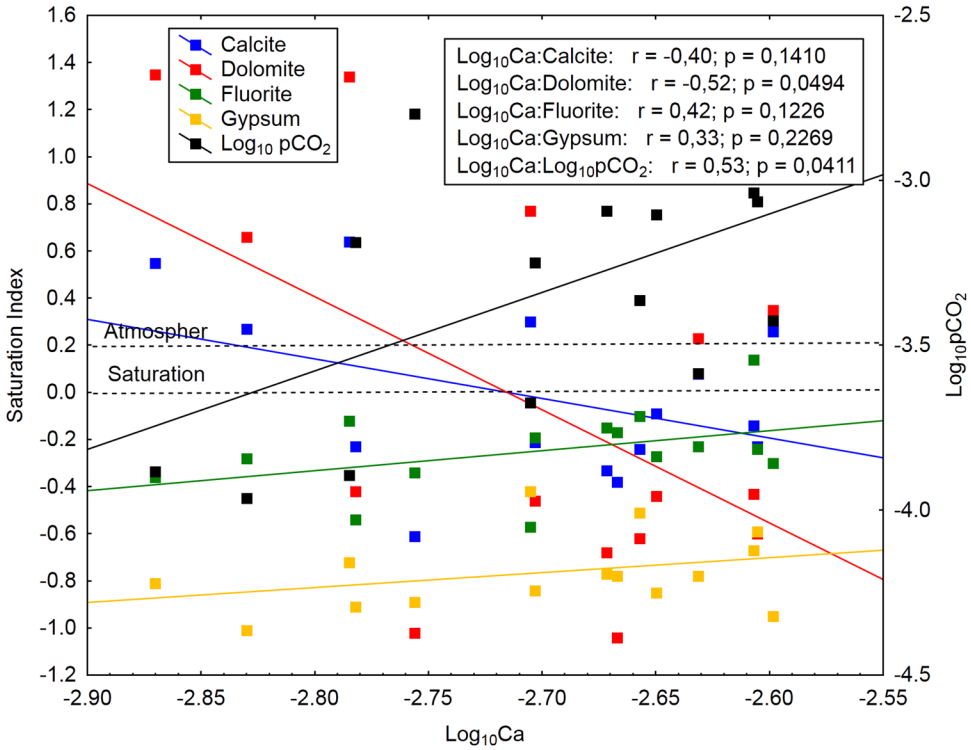

Fig. 6 Evolution of the saturation index with respect to Ca-minerals and partial pressure of CO_2 (pCO_2)

clarify water mineralization origin without investigating solid phase (Deutsch 1997). Saturation index appears to be a solution to track the fluoridation origin in studied groundwater. Fluorite (CaF_2) is often considered to be a source of fluoride in waters. Considering the equilibrium equation is written as the following:

$$Ca^{2+} + 2F^{-} \leftrightarrow CaF_2$$

$$LogK_{Fluorite} = -10,60 \text{(Phreeqc.v.3, Parkhurst and Appelo 2013).}$$

Note that thermodynamic studies indicate that F^- concentration in waters depends upon the state of equilibrium with regards to fluorite (Travi 1993). If water is undersaturated with respect to fluorite, the F^- content in the water therefore reflects its concentration in leaching rocks. Whereas if the water is saturated with respect to fluorite, the concentration of F^- would be lower and is governed by the solubility constant value of fluorite dissolution ($K_{Fluorite}$). In the studied samples, the precipitation of calcite and dolomite increase F^- activity when pH is somewhat alkaline that decreases consequently Ca^{2+} in solution. Consequently, Fluorite is leached together with gypsum and anhydrite leading to compensate Ca^{2+} as suggested by (Subba Rao et al. 2013). The precipitation of calcite and dolomite enhance dissolution Ca-bearing minerals such as fluorite that consequently increase fluoride concentration in water. In addition, the chemical activity evolution of fluoride is not only depending on the equilibrium of water with respect to carbonate minerals (Fig. 7). For instance, the speciation of fluoride in the studied water shows that the total concentration of fluoride reveals a dominance of F^- associated with MgF^+ and NaF complexes. We denote low correlation ration between $Log_{10}MgF^+$ and pH ($r = 0.33$) but more significant than that between $Log_{10}F^-$ and pH. To sum up, these results indicate the influence of carbonate (calcic and magnesian) on calcium origin reflecting the geological source of fluoride.

Spatial distribution using indicator kriging

(a) Indicator transformation and variography

Indicator kriging (IK) is highly recommended to study the fluoride distribution in CT aquifer than other interpolation methods that require a large database, good spatial distribution and some precondition of the distribution of data (e.g. ordinary kriging, Jang et al. 2008). Note that IK is largely used to carry out probability maps for pollution elements such as nitrates and other elements (e.g. Bettahar et al. 2010; Arslan 2012). It is also used to map the spatial distribution of health risk for metallic elements in aquifers (e.g. Belkhiri et al. 2017) where authors emphasize the use of IK to highlight risk probability regarding selected thresholds. For our investigation; we suggest a mapping for fluoride distribution using a fluoride threshold of 2.1 m/l. This selected value represents the median value of fluoride content in CT aquifer. Note that the median is commonly used to set the threshold by many authors (e.g. Isaaks and Srivastava 1989; Badel

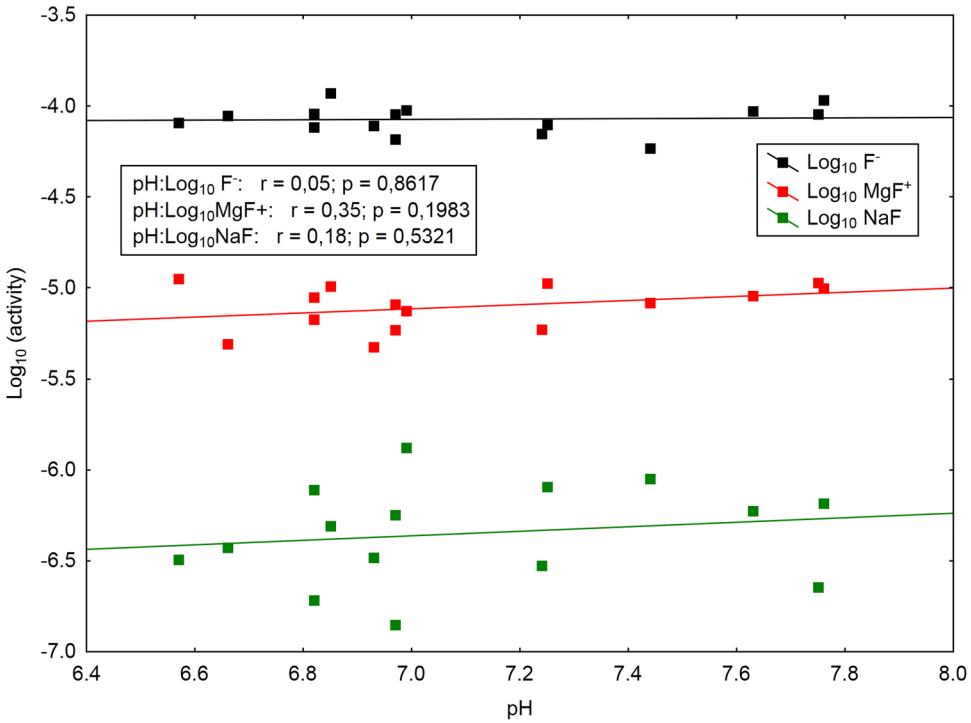

Fig. 7 Speciation of fluoride species and their evolution regarding pH in the studied water

et al. 2011; Mohammadpour et al. 2019). This selected threshold value for this study represents a critical content of fluoride in drinking water in which dental and skeletal fluorosis may substantially accelerate.

The transformation of fluoride data to indicator values according to the median threshold (Me = 2.1 mg/l) is performed. The Omnidirectional experimental variogram of the new indicator value for the selected threshold is calculated and fitted using Variowin 2.1 Software that helps in choosing the best fit found regarding goodness parameters. The PREVAR2D. VARIO2D and MODEL are the main programs used in this variability study (Pannatier 1996). Experimental variogram was fitted by spherical model with the following parameters (range = 1794 m; sill = 0.168; nugget effect = 0.111) (Fig. 8). Nugget-sill ratio for the selected threshold is 0.66 indicating strong spatial dependence (Cambardella et al. 1994; Belkhiri et al. 2017).

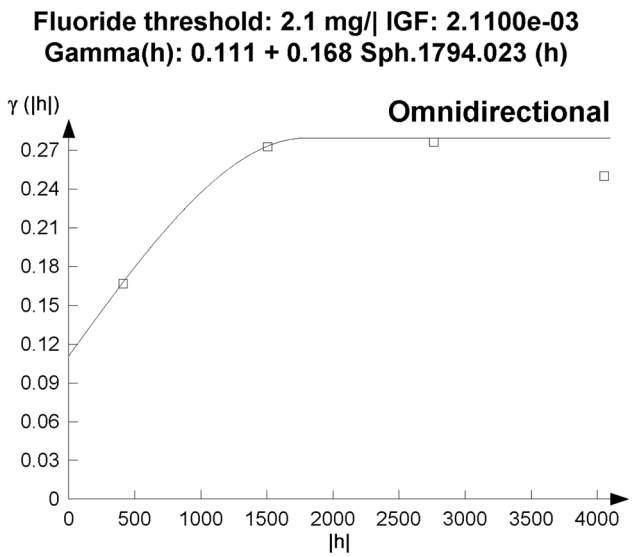

Fig. 8 Omnidirectional experimental and theoretical variogram for indicator values of fluoride (2.1 mg/l)

(b) Fluoride probability map

Using variography results, the probability map for not exceeding the selected threshold of fluoride is generated by IK procedure. We denote that the performance of this estimation method was examined by several cross-validation parameters that are given with the obtained map together with IK variance (Fig. 9). These parameters are much lower such as ME and RMSE which are found close to zero (ME = 0.0546; RMSE = 0.2). They show an accuracy of prediction as well as indicating the excellent quality of variogram fitting and good quality of estimation (Sun et al. 2009; Arslan 2012). The spatial distribution map using IK results was performed to generate a probability map of not exceeding the selected threshold, and is presented in two dimensions showing a local estimation of square mesh gridding of (250 m * 250 m). Computed probabilities of not exceeding fluoride threshold (2.1 mg/l) were grouped

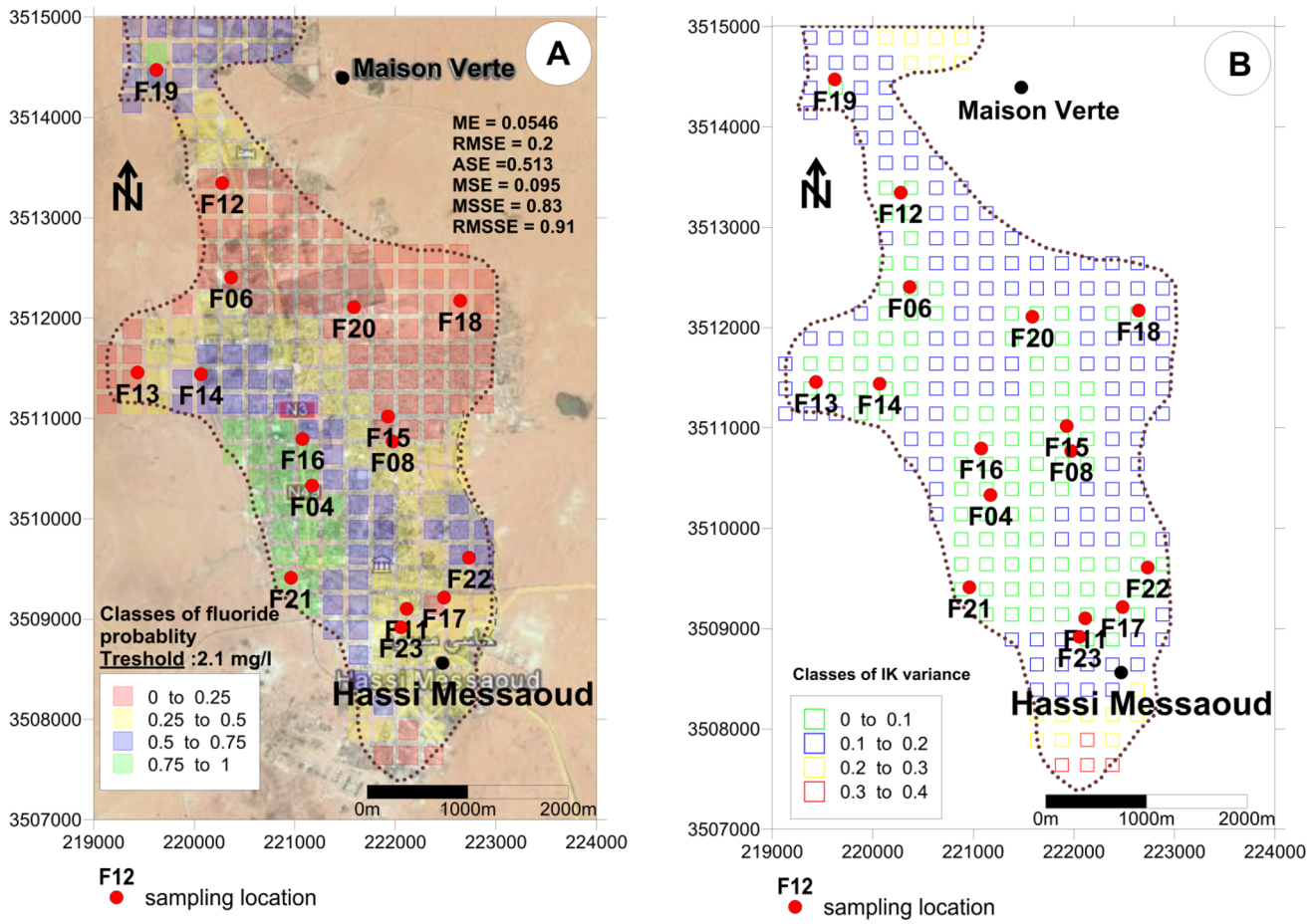

Fig. 9 **a** Spatial variability of the probability of not exceeding fluoride threshold (2.1 m/l) and cross-validation parameters in the studied aquifer, **b** map of IK variance showing lower values

into four classes: (0–0.25; 0.25–0.5; 0.5–0.75 and 0.75–1) allowing the classification of fluoride risk in investigated aquifer (Fig. 9a). The variance of IK estimation is lower showing values between zero and 0.2 (Fig. 9b). The mapping of these results shows a strong probability (≥ 0.75) of not exceeding the selected threshold value of fluoride in a limited area to the southwest part of Hassi Messaoud city representing only 10% of the investigated area. Moderate to strong probability (0.25–0.75) is observed in the central part of the study area, and low probability (0–0.25) is located in the northeastern part of Hassi Messaoud CT aquifer. In sum, moderate and low probability of not exceeding 2.1 mg/l represents 90% of the studied aquifer. Therefore a defluoridation of groundwater is highly recommended for drinking water. This map can further be used in the management of water supply to reduce the fluoride excess in drinking water on the one hand and helps decision-making for selecting the ideal position to drill new wells for water supply on the other one hand.

Conclusion

This study discusses fluoride-bearing groundwater in an arid region (Hassi Messaoud, southern Algeria) where the daily intake of water is important especially in the summer period. The hydrochemical investigation was conducted to identify the chemical characteristics of Complex Terminal groundwater and fluoride origin, whereas its spatial distribution in the aquifer has been established based on a non-linear geostatistical method of indicator kriging (IK). The main conclusions of this piece of work are the following:

(1) Fluoride concentration in the studied aquifer from the Hassi Messaoud Complex Terminal aquifer is relatively high and is largely exceeding the OMS standards for drinking water (from 1.6 to 2.9 mg/l; average = 2.1 ± 0.4 mg/l).
(2) PCA helps in identifying chemical associations of investigated water indicating high mineralization of

groundwater that is originated mainly by leaching of evaporite minerals.

(3) Saturation indices (SI) of main minerals show that waters are undersaturated with respect to evaporite minerals (anhydrite, gypsum and halite) indicating their dissolution, whereas SI of carbonates minerals (calcite and dolomite) are saturated to oversaturated reflecting their precipitation. The saturation of water regarding carbonate minerals in slightly alkaline pH enhances the dissolution of fluorite minerals to compensate Ca^{2+} in water.

(4) The use of the nonlinear geostatistical method of IK allows computing a probability map of not exceeding a selected threshold in which the median value of fluoride content (2.1 mg/l) was taken as a threshold for this study. The method consists in transforming fluoride data into a binary coding (0.1) according to the selected threshold.

(5) IK estimation was examined by cross-validation showing a high performance of the interpolation process and good quality of variogram fitting. IK estimation in square mesh gridding of (250 m * 250 m) indicates a low probability of not exceeding (2.1 mg/l) in the whole studied aquifer excepting a limited zone which represents only 10% of the studied aquifer. The obtained map can provide help for decision-making in water management and for selecting the ideal position to drill new wells for supplying drinking water.

Acknowledgements The authors would like to thank the National Water Resources Agency (ANRH) – Directorate of South-Ouargla and the Algerian Waters (ADE) – Ouargla for the fieldwork support, laboratory analyses and for providing some data used in this study. This article is a part from a National Research Project: PRFU under the Number: E04N01UN300120180002.

Compliance with ethical standards

Conflict of interest All authors have no conflicts of interest to disclose.

References

Arslan H (2012) Spatial and temporal mapping of groundwater salinity using ordinary kriging and indicator kriging: the case of Bafra Plain, Turkey. Agric Water Manag 113:57–63. https://doi.org/10.1016/j.agwat.2012.06.015

Ashrafzadeh A, Roshandel F, Khaledian M (2016) Assessment of groundwater salinity risk using kriging methods: a case study in northern Iran. Agric Water Manag 178:215–224. https://doi.org/10.1016/j.agwat.2016.09.028

Badel M, Angorani S, Shariat M (2011) The application of median indicator kriging and neural network in modeling mixed population in an iron ore deposit. Comput Geosci 37:530–540. https://doi.org/10.1016/j.cageo.2010.07.009

Belkesier MS, Zeddouri A, Halassa Y, Kechiched R (2018) Characterization and geostatistical mapping of water salinity: a case study of terminal complex in the Oued Righ Valley (Southern Algeria). AIP Conf Proc 1968:030027. https://doi.org/10.1063/1.5039214

Belkhiri L, Boudoukha A, Mouni L (2010) Groundwater quality and its suitability for drinking and agricultural use in Ain Azel plain, Algeria. J Geogr Reg Plan 3:151–157

Belkhiri L, Mouni L, Narany TS, Tiri A (2017) Evaluation of potential health risk of heavy metals in groundwater using the integration of indicator kriging and multivariate statistical methods. Groundw Sustain Dev 4:12–22. https://doi.org/10.1016/j.gsd.2016.10.003

Bettahar N, Douaoui A, Bradaï A (2010) Spatial variability of nitrate concentration in North Algeria application of ordinary and indicator kriging. Arab Water World 34:44–45

Bouselsal B (2017) Groundwater quality in arid regions: the case of Hassi Messaoud region (se Algeria). J Fundam Appl Sci 9:528–541

Cambardella CA, Moorman TB, Novak JM, Parkin TB, Karlen DL, Turco RF, Konopka AE (1994) Field-scale variability of soil properties in central Iowa soils. Soil Sci Soc Am J 58:1501–1511. https://doi.org/10.2136/sssaj1994.03615995005800050033x

Chauvet P (1999) Aide-mémoire de géostatistique linéaire. Les Presses de l'Ecole des Mines

Chilès JP, Delfiner P (1999) Geostatistics: modeling spatial uncertainty. Wiley, New York, pp 283–287

Deutsch WJ (1997) Groundwater geochemistry: fundamentals and application to contamination. Lewis Publisher, Boca Raton

Djellouli HM, Taleb S, Harrache-Chettouh D, Djaroud S (2005) Physicochemical quality of drinking water in Southern Algeria: study of excess mineral salts. Sante 15:109–112

Drever JI (1988) The geochemistry of natural waters, 2nd edn. Prentice Hall, Englewood Cliffs

Durov SA (1948) Classification of natural waters and graphical representation of their composition. Dokl Akad Nauk USSR 59:87–90

Edmunds WM, Gaye CB (1997) Naturally high nitrate baseline concentrations in groundwaters from the Sahel. J Environ Qual 26:1231–1239. https://doi.org/10.2134/jeq1997.00472425002600050006

Edmunds WM, Guendouz A, Mamou A, Moulla A, Shand P, Zouari K (2003) Groundwater evolution in the continental intercalaire aquifer of southern Algeria and Tunisia: trace element and isotopic indicators. Appl Geochem 18:805–822. https://doi.org/10.1016/S0883-2927(02)00189-0

ESRI (2008) Using ArcGIS geostatistical analyst, environmental systems. Research Institute, Redlands, CA, USA

Goovaerts P (2000) Geostatistical approaches for incorporating elevation into the spatial interpolation of rainfall. J Hydrol 228:113–129. https://doi.org/10.1016/S0022-1694(00)00144-X

Guendouz A, Moulla AS, Edmunds WM, Shand P, Poole J, Zouari JK, Mamou A (1997) Palaeoclimatic information contained in groundwaters of the Grand Erg Oriental, N. Africa. In: Isotope techniques in the study of past and current environmental changes in the hydro- sphere and atmosphere. IAEA, Vienna, pp 555–571

Guendouz A, Moulla AS, Edmunds WM (2003) Hydrogeochemical and isotopic evolution of water in the Complexe Terminal aquifer in the Algerian Sahara. Hydrogeol J 11:483–495. https://doi.org/10.1007/s10040-003-0263-7

Isaaks EH, Srivastava RM (1989) An introduction to applied geostatistics. Oxford University Press, Oxford

Jang CS, Chen SK, Ching-Chieh L (2008) Using multiple-variable indicator kriging to assess groundwater quality for irrigation in the aquifers of the Choushui River alluvial fan. Hydrol Process 22:4477–4489. https://doi.org/10.1002/hyp.7037

Journel AG (1983) Nonparametric estimation of spatial distributions. J Int Assoc Math Geol 15:445–468. https://doi.org/10.1007/BF01031292

Krige DG (1951) A statistical approach to some basic mine valuation problems on the Witwatersrand. J S Afr Inst Min Metall 52:119–139

Lee J, Jang C, Wang S, Liu C (2007) Evaluation of potential health risk of arsenic-affected groundwater using indicator kriging and dose response model. Sci Total Environ 384:151–162. https://doi.org/10.1016/j.scitotenv.2007.06.021

Lloyd CD, Atkinson PM (2001) Assessing uncertainty in estimates with ordinary and indicator kriging. Comput Geosci 27:929–937. https://doi.org/10.1016/S0098-3004(00)00132-1

Lloyd JA, Heathcote JA (1985) Natural inorganic hydrochemistry in relation to groundwater: an introduction. Oxford University Press, New York

Matheron G (1963) Principles of geostatistics. Econ Geol 58:1246–1266

Matheron G (1971) The theory of regionalized variables and its application. CAH. Cent. Morphologie Math., 5. Paris School of Mines, Fontainebleau

Messaitfa O (2008) Fluoride contents in groundwaters and the main consumed foods (dates and tea) in Southern Algeria region. Environ Geol 55:377–383. https://doi.org/10.1007/s00254-007-0983-4

Mohammadpour M, Bahroudi A, Abedi M, Rahimipour G, Jozanikohan G, Khalifani FM (2019) Geochemical distribution mapping by combining number-size multifractal model and multiple indicator kriging. J Geochem Explor 200:13–26. https://doi.org/10.1016/j.gexplo.2019.01.018

Morel FMM (1983) Principles of aquatic chemistry. Wiley, Somerset, p 446

Nezli IE, Achour S, Djidel M, Attalah A (2009) Presence and origin of fluoride in the Complex Terminal water of Ouargla Basin (Northern Sahara of Algeria). Am J Appl Sci 6:876–881. https://doi.org/10.3844/ajas.2009.876.881

Pannatier Y (1996) VARIOWIN: software for spatial data analysis in 2D. Springer, New York

Parkhurst DL, Appelo CAJ (2013) Description of input and examples for PHREEQC version 3: a computer program for speciation, batch-reaction, one-dimensional transport, and inverse geochemical calculations. U.S. Geological Survey Techniques and Methods, book 6, chapter A43. http://pubs.usgs.gov/tm/06/a43/

Rodier J (1996) L'analyse de l'eau, eaux naturelles, eaux résiduaires, eau de mer, 8th edn. Dunod, Paris

Sahri L, Nezli IE, Kechiched R, Benhamida AS (2017) A statistical summary of ground water mineralization in the aquifer of intercalary continental (Algerian Septentrional Sahara). Energy Proc 119:386–392. https://doi.org/10.1016/j.egypro.2017.07.122

Shaw PJA (2003) Multivariate statistics for the environmental sciences. Hodder-Arnold, London. ISBN 0-340-80763-6

Sonatrach (2002) La stratigraphie du champ Hassi Messaoud. Rapport interne, Division Exploration (*an internal report*)

Subba Rao N, Subrahmanyam A, Babu Rao G (2013) Fluoride-bearing groundwater in Gummanampadu Sub-basin, Guntur District, Andhra Pradesh, India. Environ Earth Sci 70:575–586. https://doi.org/10.1007/s12665-012-2142-9

Sun Y, Kang S, Li F (2009) Comparison of interpolation methods for depth to groundwater and its temporal and spatial variations in the Minqin oasis of northwest China. Environ Model Softw 24:1163–1170. https://doi.org/10.1016/j.envsoft.2009.03.009

Travi Y (1993) Hydrogéologie et hydrochimie des aquifères du Sénégal. Hydrogéologie et Hydrogéochimie du fluor dans les eaux souterraines, Sciences Géologiques, Mémoire, no. 95

UNESCO (1972) Projet ERESS: étude des ressources en eau du Sahara septentrional. Rapport final (ERESS project: study of the northern Sahara water resources. Final report), United Nations Educational Scientific and Cultural Organisation (UNESCO), Paris

WEC (2007) Well evaluation conference «WEC». SLB document

Wedepohl KH (1974) Hand-book of geochemistry, vol II-4. Springer, Berlin, p 9K-1

WHO (2017) Guidelines for drinking-water quality, 4th edition, incorporating the 1st addendum, WHO Library Cataloguing-in-Publication Data, pp 372–373

Xavier E (2001) Géostatistiques linéaire. Ecole des mines de Paris

Youcef L, Achour S (2001) Defluoruration des eaux souterraines du sud algerien par la chaux et le sulfate d'aluminium. Courrier du Savoir 1:65–71

Youcef L, Achour S (2004) Etude de l'élimination des fluorures des eaux de boisson par adsorption sur bentonite. Larhyss Journal 3:129–142